# Nano Titanium Oxide Organosol: Synthesis, Characterization, and Application for Electrorheological Fluid

**Yan Zhao, Baoxiang Wang, Changlin Ding, Xiaopeng Zhao**

*Institute of Electrorheological Technology, Department of Applied Physics, Northwestern Polytechnical University, Xi'an 710072, People's Republic of China*

Received 22 June 2006; accepted 16 December 2006
DOI 10.1002/app.27728
Published online 18 September 2008 in Wiley InterScience (www.interscience.wiley.com).

**ABSTRACT:** A liquid–liquid phase transfer method was employed to prepare novel nano titanium oxide/silicone oil organosol. First, titanium oxide nanoparticles were synthesized in aqueous phase and then modified with several surfactants. It is found that only sodium dodecyl benzene sulfonate (SDBS) and sodium dodecyl sulphate (SDS) can cap nanoparticles and then nanoparticles could be transferred into organic phase by the phase transfer method. The transfer process was certified by the rapid change of color for the aqueous and organic phase. Other surfactants including hexadecyltrimethyl ammonium bromide (CTAB) and oleic acid were unable to ensure the phase transfer in the organic phase. The procedure was also verified by high-resolution transmission electron microscopy (HRTEM), particle size analyzer, UV–vis, etc. The results also showed the narrow size distribution of the nanoparticles. The mechanism of phase transfer is also discussed for different surfactant. Because of its good antisedimentation and high electrorheological effect, organosol is a novel path for the design and application of electrorheological fluid. © 2008 Wiley Periodicals, Inc. J Appl Polym Sci 110: 3763–3769, 2008

**Key words:** organosol; phase transfer; electrorheological fluid; nanoparticle

## INTRODUCTION

Electrorheological fluids (ERFs) are usually suspensions of microscale dielectric particles dispersed in insulating oil; their rheological properties are drastically changed by an applied electric field.[1–3] The suspended particles attract each other to form fibrillation structure that result in a drastic increase of the apparent viscosity under the external electric field. This phenomenon is also reversible when external electric field is removed. The main characteristics of ER fluid are a high-yield stress and enhanced viscosity under an applied electric field, a response time on the order of milliseconds, and full reversibility.[4–13] The ERF is either heterogeneous or homogeneous. In the heterogeneous group, the dispersed particles (such as inorganic, organic, or polymeric particulate) should be prepared first and then mixed with insulating oil. Recently, Wen et al.[14] reported new electrorheological (ER) fluids consisting of nanoparticles dispersed in an insulating liquid. It remains as a heterogeneous ER fluid because a step-by-step method, including preparation of the particle, drying, mixing with insulating oil, etc., is used. As a result, agglomeration of nanoparticles and powder pollution, which is unavoidable, takes place in both steps, especially in the process of drying, storage, and transportation of nanoparticles. Homogeneous ER fluids, which is liquid crystal dispersed into insulating oil, do not have particle sedimentation problem as the heterogeneous ER fluid usually have. However, such ER fluids would not give a strong ER effect and have a longer response time, and they also have large zero field viscosity.[15] So exploring new approaches for the preparation of ERF with excellent properties are the focus of electrorheological field.

Recently, for their excellent properties in film preparation,[16–19] thermal transfer,[20] and functional material preparation,[21] organosol have attracted the interest of many researchers. A variety of nanoparticle organosol, including Au, Ag, Pt, $Y_2O_3$, CuO, etc., have been prepared by various methods,[22–27] such as liquid–liquid phase transfer method, hydrothermal method,[26] microemulsion method,[27] etc. Mayya and Caruso[28] achieved the complete phase transfer of surface-modified gold nanoparticles from the aqueous to the organic phase in the present of primary amines. Meriguet et al.[24] developed a new and reproducible method based on a surfactant-

*Correspondence to:* X.-P. Zhao (xpzhao@nwpu.edu.cn).
Contract grant sponsor: National Natural Science Foundation of China; contract grant number: 50272054.
Contract grant sponsor: National Natural Science Foundation of China for Distinguished Young Scholars; contract grant number: 50025207.

mediated liquid–liquid phase transfer of individually dispersed $\gamma$-$Fe_2O_3$ nanoparticles from an aqueous colloidal dispersion to an organic phase. He et al.[16] prepared monodisperse and stable silver nanoparticles in chloroform employing liquid–liquid phase transfer method and obtained self-assembled two-dimensional ordered superlattice, which is long-range ordering and close-packed nanoparticle arrays. Phase transfer method was widely used to prepare metal nanoparticles,[16–20,23] but few report for the preparation of inorganic oxide organosol.[24–27]

Here, we report a facile and rapid liquid–liquid phase transfer procedure for preparing nano titanium oxide organosol, which is the first time to import this method for the preparation of ERFs. By the transfer of modified nanoparticles from aqueous phase to organic phase, unwanted ions can be removed, which was helpful to reduce the leakage current density of ERFs. In the process, surface modified titanium oxide nanoparticles were prepared in concentrated HCl environment first, and then the nanoparticles were transported directly into the organic phase, which is the mixture of silicone oil and petroleum ether. After segregating with hydrosol, organosol was volatilized under room temperature to remove petroleum ether. Then the organosol ERF was obtained. Its ER and dielectric properties were also studied.

## EXPERIMENTAL

### Materials

Hydrochloric acid (Tian Jin, China, HCl), sodium dodecyl benzene sulfonate (Tian Jin BoDi Chem. Co. China, SDBS), sodium dodecyl sulfate (Tian Jin, China, SDS), hexadocyltrimethy ammonium bromide (Shang Hai, China, CTAB), butyltitanate (Tian Jin, TBT), and petroleum ether (Tian Jin, China) are all analytical reagent and used as received.

### Preparation of organosol electrorheological fluid

The synthesis route of organosol ERF is shown in Figure 1. Thirty milliliter of distilled water was placed in a 100-mL vessel and 7 mL TBT was added under magnetic stirring. After stirred 10 min, the pH value is adjusted to 0.5–1 by drop-wise addition of 6*M* hydrochloric acid solution, followed by a stirring for another 5 h in water bath under 50°C. The as prepared nano titanium oxide hydrosol was weak blue and stocked for using. Some amount of surfactant, such as SDS, was dissolved into 10-mL distilled water and then added to the as prepared nano titanium oxide hydrosol in a 100-mL vessel. After the suspension was stirred 3 h at room temperature, the organic phase 60 mL petroleum ether containing 6 mL silicone oil (dielectric constant $\varepsilon_f$ = 2.60–2.80, conductivity

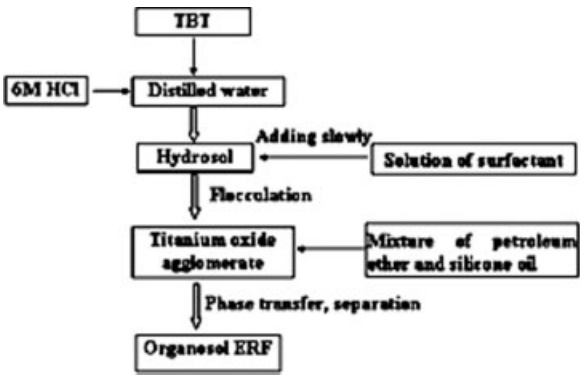


**Figure 1** Flow chart for the preparation of organosol ERF.

$\sigma_f = 10^{-12}$–$10^{-13}$ S/m, density $\rho$ = 0.9–1.0 g/cm$^3$, viscosity $\eta$ = 50 mPa · s) was added. The mixture was vigorous stirred 5 h. Then with the help of separating funnel, the milk white layer was separated from the completely colorless aqueous layer, showing the nano titanium oxide had been successfully transferred from the aqueous to the organic phase.[29] After segregating with hydrosol, organosol was volatilized under room temperature to remove petroleum ether. Then the organosol ERF was obtained.

### Characterization

A Malvern Zetasizer Nano-Zs particle size analyzer (UK, Malvern) was used to obtain particle size distributions. The phase transfer phenomenon was exhibited by the digital camera photos. UV–vis spectra are recorded with a UV-9100 spectrophotometer (Beijing Rayleigh analytical instrument Corporation, China) in range of 200–800 nm, with a resolution of 5 nm. TEM (JEM2010, JEOL, Japan) was used to observe the morphology and size of titanium oxide colloid particles under 200 kV.

Dynamic shear stress and temperature effect of as prepared electrorheological fluid are measured with a Haake RS600 (Agilent, USA) electrorheological meter with a plate–plate system (PP 35ER), a WYZ-010 DC high-voltage generator, an oil bath for temperature control, and a PC computer. The flow curves were measured by the controlled shear rate (CR) mode in the shear rate from 1 to 1000 s$^{-1}$. The dielectric relaxation spectra of ER fluid were measured by a 4284A precision LCR meter analyzer (Agilent, USA) using a 16452A measuring fixture (Agilent, USA). The AC electrical field within 20 Hz–1 MHz was applied to the ER fluid during measurement.

## RESULTS AND DISCUSSION

Previous works indicate that surfactant is essential for a particular solvent system.[30] The category, HLB value, and dosage of surfactant obviously influence

**TABLE I**
**Experimental Phenomena for Different Surfactants**

| Surfactant category | Precipitate phenomenon | Change of hydrosol | Phase transfer phenomenon |
|---|---|---|---|
| Oleic acid (nonionic) | Not obvious | Slight turbid | Separated into two layers [Fig. 2(a)] |
| CTAB (cationic) | Not obvious | Transparent | No separation [Fig. 2(b)] |
| SDBS (anionic) | Faster | Precipitate on the bottom | Separated into two layers [Fig. 2(d)] |
| SDS (anionic) | Faster | Precipitate on the bottom | Separated into two layers [Fig. 2(c)] |

the phase transfer efficiency of metal oxide. Representative surfactants, including oleic acid (nonionic), CTAB (cationic), SDBS (anionic), and SDS (anionic), have been used as phase transfer agent to prepare nano titanium oxide organosol; the concentration of surfactant is $3.45 \times 10^{-2}M$. Table I and Figure 2 show experiments phenomenon when different species surfactant was used. Organosol would not be obtained for using oleic acid [Fig. 2(a)] and CTAB [Fig. 2(b)] as phase transfer agent. When oleic acid was added, there is no phase precipitation in hydrosol and no phase separation after organic phase was added. Cationic surfactant CTAB emulsifies the mixture of aqueous and organic phase and also no phase separation occur. Anionic surfactant was found to get a better phase transfer, both SDBS and SDS precipitate the hydrosol and there is an obvious layer separation. Figure 2(c,d) show that SDS have a better phase transfer efficiency than SDBS. The reason will be discussed later.

The influence of surfactant concentration on phase transfer efficiency was also studied. Figure 3 shows that there is an optimum dosage of SDS, too little surfactant result in low phase transfer efficiency, and too much surfactant emulsify the mixture of aqueous and organic phase.

## Mechanism

Experimental show that the category of surfactant was essential to the phase transfer. It is commonly agreed that cationic nanosized titanium oxide with narrow particle size distribution could be obtained under highly acidic environment. Oleic acid could affiliate on titanium oxide surface depending on van der Waals attraction. But owing to the low solubility in aqueous, there is no sufficient oleic acid available to affiliate on titanium oxide surface. The particles are still hydrophilic and the phase transfer is unsuccessful. When SDS or SDBS were added, anionic head of surfactant affiliate on the cationic nanoparticles through electrostatic interaction and the hydrophobic tail extend out. There is an optimum amount of SDS and SDBS, when SDS was deficient, surface modification is not fully attained, and the phase transfer is incomplete. Along with the sequential addition of surfactant, a single surfactant molecule layer was probably formed and the best phase transfer attained (see Fig. 4). On the other hand, when it is excess, the second surfactant molecule layer begin to form through van der Waals attraction which the

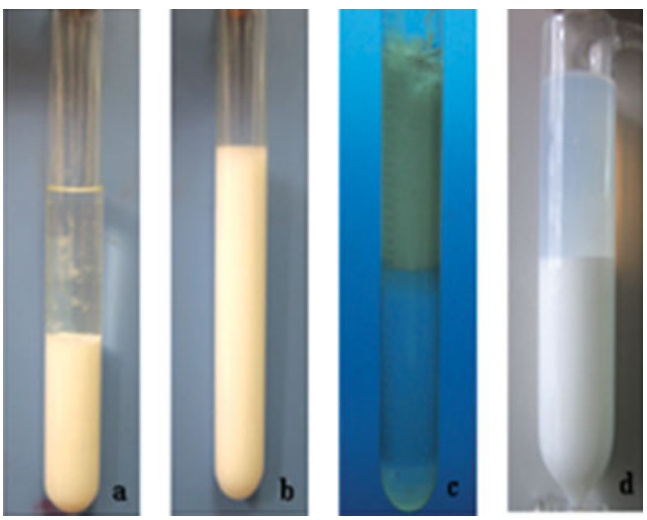


**Figure 2** Photos of phase transfer effect when different surfactants were used. (a) Oleic acid; (b) CTAB; (c) SDS; (d) SDBS. [Color figure can be viewed in the online issue, which is available at www.interscience.wiley.com.]

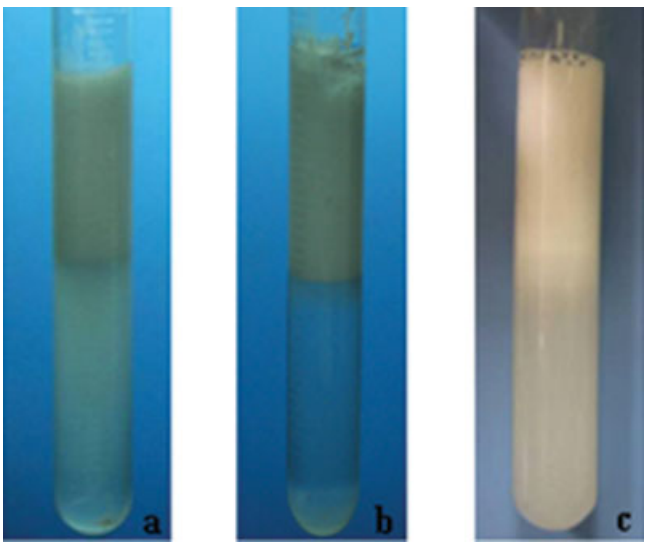


**Figure 3** Effect of SDS dosage on the phase transfer. (a) $2.12 \times 10^{-2}M$; (b) $3.45 \times 10^{-2}M$; (c) $4.96 \times 10^{-2}M$. [Color figure can be viewed in the online issue, which is available at www.interscience.wiley.com.]

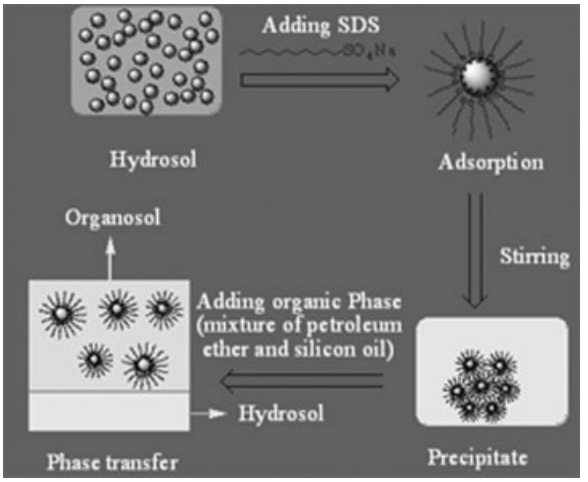


**Figure 4** Schematic diagram of action mechanism of SDS.

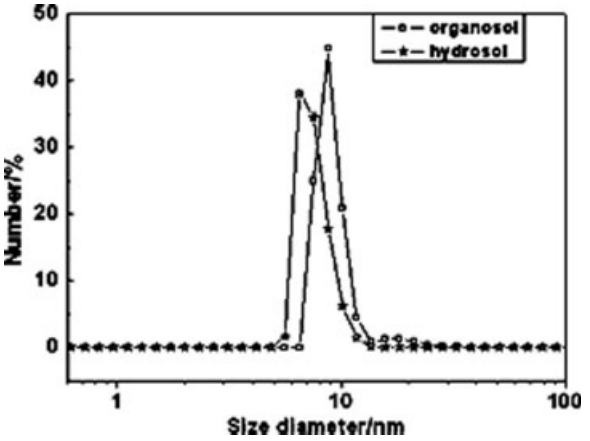


**Figure 6** Particle size distribution of as prepared hydrosol and organosol.

surfactant tail affiliate on the modified nanoparticles and the nanoparticles become hydrophilic.

The HLB value also has an effect on phase transfer, under the same experiment conditions, SDS which has a high HLB value of 40 results in a high transfer effecting than that of SDBS which has a HLB value of 20.

When CTAB was used, under the simultaneously action of electrostatic repulse action and van der Waals attraction, the hydrophobic tails of CTAB absorb on the particles and hydrophilic head extend out, so the particles are still hydrophilic.

Figure 5 shows the UV–vis spectra of as prepared titanium oxide hydrosol and organosol. Figure 5(a) shows that there was no significant optical absorption peaks in the visible region. Both the different solutions have high absorption [Fig. 5(a)] in short wavelength and transmittance [Fig. 5(b)] in long wavelength. The absorption edges for as prepared titanium oxide nanoparticles show a red shift from 350 to 369 nm upon the transfer from water to the mixture of petroleum ether and silicone oil, showing the particle grow bigger on the transfer process. Those are consistent with the results of particle size distribution showing in Figure 6. The transmittance of hydrosol in the visible range is better than that of organosol [Fig. 5(b)]. Average particle size of the hydrosol and organosol are 7.5 and 9.4 nm separately as showing in Figure 6, and they both have a narrow particles distribution. Morphology and size of the titanium oxide colloid particles in hydrosol and organosol were also evaluated by their HRTEM micrograph, which are white particles shown in Figure 7. They are being nearly spherical in shape and exhibiting a rather uniform size distribution.

### Rheological properties of the organosol ERF

Flow curves were measured using CR mode for titanium oxide organosol ERF under different electric

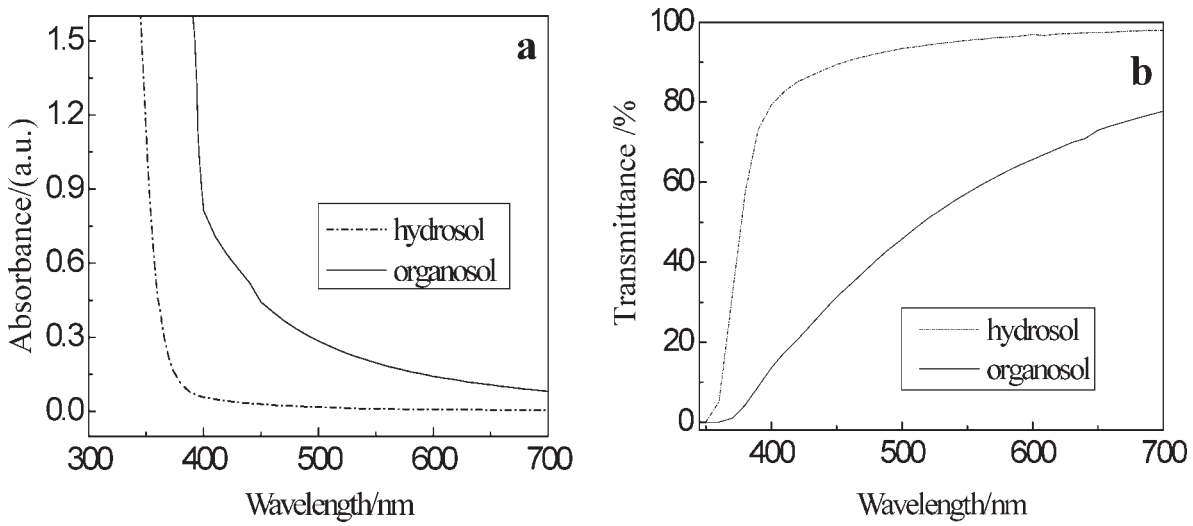


**Figure 5** UV–vis spectra of as prepared hydrosol and organosol. (a) absorbance; (b) transmittance.

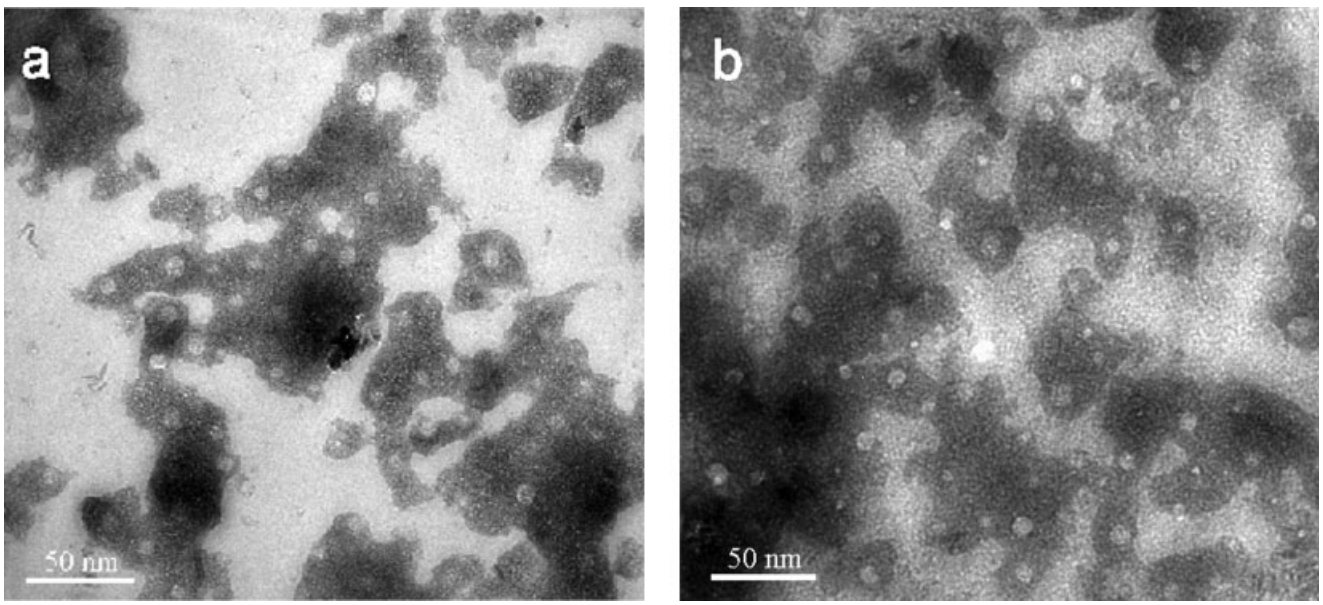


**Figure 7** HRTEM images of (a) hydrosol and (b) organosol.

field strengths, as shown in Figure 8. In the absence of an electric field, the organosol ERF behaves as a Newtonian fluid, whose shear stress increases linearly with shear rate with a slope of 0.8. When a DC electric field is applied, as the shear rate increases, the behavior of shear stress only decreased slightly even at very high shear rate and shows a Bingham fluid behavior. This behavior is described by the following Bingham fluid model in general,

$$\begin{cases} \begin{cases} \tau = \tau_y + \eta\dot{\gamma} & if\, \tau \geq \tau_y \\ \dot{\gamma} = 0 & \text{if } \tau \geq \tau_y \end{cases} \end{cases} \quad (1)$$

Here, $\tau_y$ is the yield stress and is a function of an electric field strength, $\tau$ is the shear stress, $\dot{\gamma}$ is the shear rate, and $\eta$ is the shear viscosity. The yield stress, the critical parameter in ER response, depends on the electrical field strength and particle volume fraction. It is known that the rheological behavior of an ER suspension is the result of a change of fibrous-like structures. This structure change is mainly dominated by the electric-field induced electrostatic interaction and the shear-field-induced hydrodynamic force. The large polarizability and enough polarization response of ER particles are important to produce stronger and faster electrostatic interaction that can maintain structures and rheological properties stable under shear flow. As we increase the shear rate, the fibrillar structure of particles aligned in the applied electric field direction is distorted and destroyed via an imposed strain. However, the shear stress remained approximately constant (plateau region) as the shear rate increased (see Fig. 8), where the electrostatic force becomes approximately enough to the hydrodynamic force. The stable shear stress level for the organosol ERF means that the electrostatic interaction and the polarization response are still enough even if the shear rate is increased, and thus, particles make fibrous structures fast enough to maintain the structure and rheological properties under shear flow. Figure 9 shows the apparent viscosity of the organosol ERF as a functional of shear rate at different electric field in a range of shear rate from 1 to $10^3$ $s^{-1}$. It shows the apparent viscosity of the organosol ER fluid is relatively low at zero fields, and upon the application of the electric field, a shear-dependent viscosity that decrease with the increasing shear rate is observed, similar to shear thinning behavior found in polymer melts or solutions.[31] The viscosity increases by 2 or 3 orders of magnitude at a

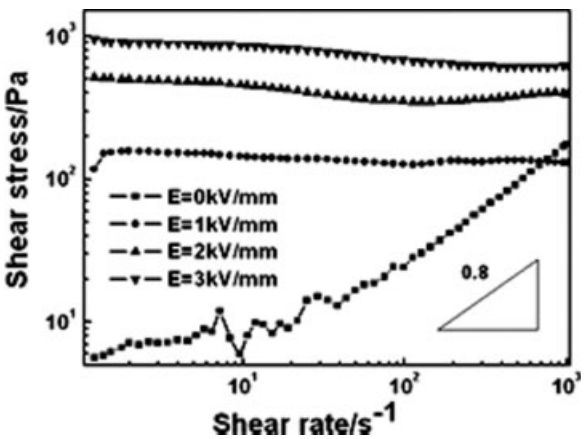


**Figure 8** Shear stress as a function of shear rate for as prepared titanium oxide organosol ERF under different electric field.

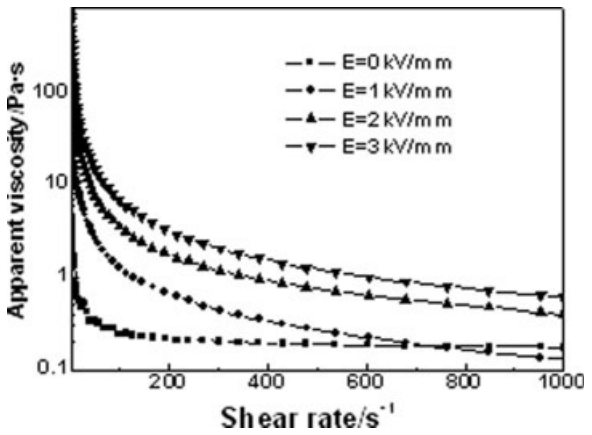


**Figure 9** Apparent viscosity as a function of shear rate for as prepared titanium oxide organosol ERF under different electric field.

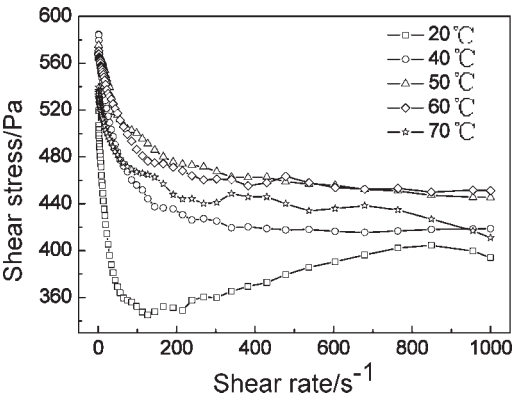


**Figure 10** Shear stress versus shear rate for as prepared titanium oxide organosol ERF at different temperature ($E$ = 2 kV/mm).

low shear rate region, which means that the fluid is strongly solidified under electric field (see Table II). Figures 8 and 9 show an obvious ER effect, which the shear stress and apparent viscosity increasing quickly with increasing electric field strength due to the enhanced interparticle interactions. Under the electric field strength of 3 kV/mm, the ER efficiency $\eta_E$ ($\eta_E = (\tau_E - \tau_0)/\tau_0$, where $\tau_E$ is the shear stress with electric field and $\tau_0$ is the shear stress without electric field) is close to 15 at the shear rate of 200 $s^{-1}$. Leakage current density was also measured less than 5 $\mu A/cm^2$.

Figure 10 shows the shear stress versus shear rate of as prepared organosol ERF at different temperature, which the electric field strength is 2 kV/mm. The ER effect of the organosol is better from 20 to 70°C. The shear stress increase with temperature and reach maximum around 60°C.

The dielectric spectra of the titanium oxide ERF in the frequency range from 10 to $10^6$ Hz were measured using LCR meter analyzer. The dielectric constant and dielectric loss factor of the as prepared organosol ERF as a function of frequency are given in Figure 11.

The interfacial polarization mechanism treats particle polarization using complex dielectric constant $\varepsilon = \varepsilon' - i\varepsilon''$, where $\varepsilon'$(dielectric constant) is related to particle polarizability and $\varepsilon''$(dielectric loss factor) is related to polarization time and stability of interaction between particles. Block[32–35] et al. proposed a good ER effect require the suspension should first have a dielectric relaxation peak ($\varepsilon''$) in the range from $10^2$ to $10^5$ Hz and should have a large $\Delta\varepsilon$ where $\Delta\varepsilon' = \varepsilon'_{10^5\text{Hz}} - \varepsilon'_{10^2\text{Hz}}$. For our samples, $\Delta\varepsilon$ (about 4) was observed in the organosol as shown in Figure 11. It also have a relaxation peak at 200 Hz, which in the range of $10^2$–$10^5$ Hz. Interfacial polarization can be affected by the flow field so that the ER phenomenon is the result of the interaction between the flow field and the polarization induced by the external electric field.[24] The dielectric relaxation time $\tau$ of the polarization for the organosol can be obtained from the relation $\tau = 1/2\pi f_{max}$, where $f_{max}$ is the local frequency of the $\varepsilon''$ peak. Figure 11 shows the organosol dielectric loss peak around $f_{max}$ = 200 Hz; thus, the large $\Delta\varepsilon'$ and proper polarization response in the organosol induce a strong and stable interaction between particles leading to a good ER effect, as shown in Figure 8.

The above discussion can also explain the flow behaviors in Figure 8. As shown in Figure 8,

**TABLE II**
**Apparent Viscosity at Zero Shear Rate Under Different Electric Field**

| Parameters | $E$ =1 kV/mm | $E$ = 2 kV/mm | $E$ = 3 kV/mm |
|---|---|---|---|
| Apparent viscosity (Pa s) | 114.5 | 482.5 | 822.3 |

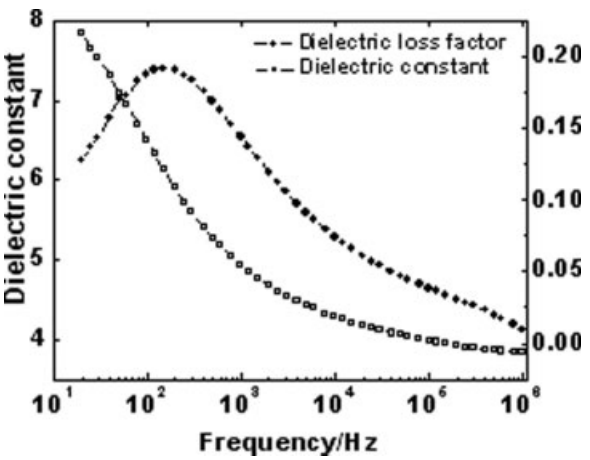


**Figure 11** Permittivity and dielectric loss factor of as prepared organosol ERF as a function of the frequency.

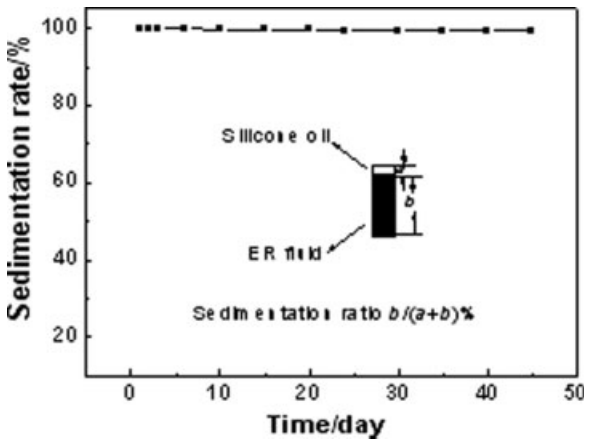


**Figure 12** The sedimentation ratio of organosol ERF versus time.

especially in the shear rate above 100 $s^{-1}$, the relaxation time ($\approx 10^{-3}$ s) is shorter than the inverse shear rate of the shear field. The polarization of the organosol can sustain with the external electric field, so that the shear stress remains constant. In conclusion, the better ER performance can be explained from the dielectric spectra.

Sedimentation is one of main criteria used to evaluate whether the materials can be commercialized or not, because the properties of ERFs should be weaken rapidly with the sedimentation of the particle phase. Figure 12 shows the sedimentation ratio of the organosol. According to Figure 12, the as prepared organosol have an excellent antisedimentation stability, which the sedimentation ratio is 99.3% over 45 days. The good sedimentation can attribute to the small size distribution of the titanium oxide colloid nanoparticles.

## CONCLUSIONS

Liquid–liquid phase transfer method has been successfully introduced to fabricate novel nano titanium oxide/silicone oil organosol that shows excellent ER effect. The surfactant species was critical to the phase transfer. Oleic acid and CTAB were unable to ensure the phase transfer in the organic phase. Anionic surfactant SDS and SDBS can bring a good layer separation and SDS possessed a larger HLB value has a good phase transfer effect. The complete phase transfer was thought to base on the attractive electrostatic interaction between the negative charged surfactant group and the positive charged nanoparticle. There is an optimum dosage of SDS 3.45 $\times 10^{-2} M$. When SDS is deficient, good phase transfer efficient can not be attained. On the other hand, when SDS is excess, the redundant SDS emulsify the mixture. The average particle size of as prepared organosol and hydrosol are 7.5 and 9.4 nm, respectively. The organosol exhibits good ER effect that the ER efficiency is above 15 under a shear rate of 200 $s^{-1}$ and the leakage current density is less than 5 $\mu A/cm^2$. The organosol also show a good ER effect in a broad temperature range of 20–70°C. The stronger polarization is the origin of the good ER effect.

## References

1. Block, H.; Kelly, J. P. J Phys D: Appl Phys 1988, 21, 1661.
2. Whittle, M.; Blullough, W. A. Nature 1992, 358, 373.
3. Halsay, T. C.; Matin J. E. Science 1992, 258, 761.
4. Hao, T. Adv Mater 2001, 13, 1847.
5. Gamota, D.; Filisko, F. E. J Rheol 1991, 35, 399.
6. Wang, B. X.; Zhao, X. P. Adv Funct Mater 2005, 15, 1815.
7. Wang, B. X.; Zhao, X. P. Langmuir 2005, 21, 6553.
8. Yin, J. B.; Zhao, X. P. Chem Mater 2004, 16, 321.
9. Wang, B. X.; Zhao, X. P. J Mater Chem 2003, 13, 2248.
10. Zhao, X. P.; Yin, J. B. Chem Mater 2002, 14, 2258.
11. Sim, I. S.; Kim, J. W.; Choi, H. J.; Kim, C. A.; Jhon, M. S. Chem Mater 2001, 13, 1243.
12. Cho, M. S.; Choi, H. J.; Kim, K. Y.; Ahn, W. S. Macromol Rapid Commun 2002, 23, 713.
13. Cho, M. S.; Choi, H. J.; Ahn, W. S. Langmuir 2004, 20, 202.
14. Wen, W. J.; Huang, X. X.; Yang, S. H.; Lu, K. Q.; Sheng, P. Nat Mater 2003, 2, 727.
15. Inoue, A.; Mannewa, S. J Appl Polym Sci 1995, 55, 113.
16. He, S.; Yao, J. N.; Jiang, P.; Shi, D. X.; Zhang, H. X.; Xie, S. S.; Pang, S. J.; Gao, H. J. Langmuir 2001, 17, 1571.
17. Rao, C. N. R.; Kulkarni, G. U.; Thomas P. J.; Agrawal, V. V.; Saravanan, P. J Phys Chem B 2003, 107, 7391.
18. Zhao, S. Y.; Wang, S. H.; Kimura, K. Langmuir, 2004, 20, 1977.
19. Chauhan, B. P. S.; Sardar, R. Macromolecules 2004, 37, 5136.
20. Zhu, H. T.; Lin, Y. S.; Yin, Y. S. J Colloid Interface Sci 2004, 277, 100.
21. Wilson, O.; Wilson, G.J.; Mulvaney, P. Adv Mater 2002, 14, 1000.
22. Prasad, B. L. V.; Arumugam, S. K.; Bala, T.; Sastry, M. Langmuir 2005, 21, 822.
23. Zhao, S. Y.; Chen, S. H.; Wang, S. Y.; Li, D. G.; Ma, H. Y. Langmuir 2002, 18, 3315.
24. Meriguet, G.; Dubois, E.; Perzynski, R. J Colloid Interface Sci 2003, 267, 78.
25. Yoshitake, K.; Koyama, Y.; Suemura, N. U.S. Pat. 0050154124 (2005).
26. Wang, X.; Zhuang, J.; Peng, Q.; Li, Y. D. Nature 2005, 437, 121.
27. Wang, J. X.; Dong, X. T.; Yan, J. H.; Fan, X. Z.; Feng, X. L.; Hong, G. Y. J Rare Earths 2004, 22, 140.
28. Mayya, K. S.; Caruso, F. Langmuir 2003, 19, 6987.
29. Zhao, X. P.; Zhao, Y.; Wang, B. X. China Pat. 200510096105.2 (2005).
30. Tarasanhkar, P.; Tapan, K. S.; Nokhil, R. J. J Colloid Interface Sci 1998, 202, 30.
31. To, K.; Choi, H. J. Phys Rev Lett 1998, 80, 536.
32. Block, H.; Kelly, J. P.; Qin, A. Watson, T. Langmuir 1990, 6, 6.
33. Hao, T.; Kawai, A.; Ikzaki, F. Langmuir 1998, 14, 1256.
34. Ikzaki, F.; Kawai, A.; Uchida, K.; Kawakami, T.; Edmura, K.; Sakurai, K.; Anzai, H.; Asako, Y. J Phys D: Appl Phys 1998, 31, 336.
35. Kawai, A.; Ide, Y.; Inoue, A.; Ikzaki, F. J Chem Phys 1998, 109, 4587.